Analysis of Entrance and Exit Effects in a Falling Cylinder Viscometer

M. C. S. CHEN and G. W. SWIFT

Department of Chemical and Petroleum Engineering
The University of Kansas, Lawrence, Kansas

A variational method has been used to study the entrance and exit effects in a falling cylinder viscometer for creeping and noncreeping flow. The computed results indicate solution convergence for N_{Re} less than 100 and agree with experiment within ± 0.5% for N_{Re} less than 25.

Theoretical studies to date on the falling cylinder viscometer (*1, 3, 5, 8*) assumed that entrance and exit effects could be neglected. Thus, experimentalists employing the falling cylinder viscometer (*6, 10, 11*) found it necessary to calibrate their viscometers to compensate for entrance and exit effects.

This paper presents the development and solution of equations for incompressible, Newtonian fluid flow in the falling cylinder viscometer including entrance and exit effects, and experimental data corroborating the calculated results for $N_{Re} < 25$.

THEORY

For a steady, axisymmetric flow of an isothermal, incompressible, Newtonian fluid with the assumption that $p = f(z)$ only, the equations of continuity and motion in cylindrical coordinates are:

$$\frac{1}{r}\left[\frac{\partial r v_r}{\partial r}\right] + \frac{\partial v_z}{\partial z} = 0 \tag{1}$$

$$\rho\left[v_r\frac{\partial v_r}{\partial r} + v_z\frac{\partial v_r}{\partial z}\right] = \mu\left[\frac{\partial}{\partial r}\left[\frac{1}{r}\frac{\partial r v_r}{\partial r}\right] + \frac{\partial^2 v_r}{\partial z^2}\right] \tag{2}$$

$$\rho\left[v_r\frac{\partial v_z}{\partial r} + v_z\frac{\partial v_z}{\partial z}\right] = -\frac{\partial p}{\partial z} + \rho g_z + \mu\left[\frac{1}{r}\frac{\partial}{\partial r}\left[r\frac{\partial v_z}{\partial r}\right] + \frac{\partial^2 v_z}{\partial z^2}\right] \tag{3}$$

Under the further assumption that entrance and exit effects are negligible, Lohrenz (*8*) determined that for a falling cylinder of radius κR, moving in the negative z direction through a tube of radius R filled with fluid:

$$\frac{\mu v_0}{(\sigma - \rho)g} = \beta_0 = \frac{(\kappa R)^2}{2}\left[\ln(1/\kappa) + (\kappa^2 - 1)/(\kappa^2 + 1)\right] \tag{4}$$

To consider the solution of Equations (1), (2), and (3) for the falling cylinder viscometer with end effects, it is convenient to do so without computing the pressure distribution in the flow domain. Define

$$\frac{\mu v_1}{(\sigma - \rho)g} = \frac{(\kappa R)^2}{2\overline{F}_k} = \frac{1}{2L}\left[\frac{\kappa R}{v_1}\right]^2 \int\int \Phi_v{}'\, r dr dz \tag{5}$$

where

$$\Phi_v{}' = 2[(\partial v_r/\partial r)^2 + (v_r/r)^2 + (\partial v_z/\partial z)^2] + (\partial v_r/\partial z + \partial v_z/\partial r)^2 \tag{6}$$

[see Bird et al. (*2*), p. 91]. Then

$$\frac{v_1}{v_0} = \frac{(\kappa R)^2}{2\overline{F}_k\beta_0} = \Psi_{ee} \tag{7}$$

The problem then, is to compute $\overline{F}_k$ so that the terminal velocity can be corrected for end effects.

Theoretically, the fluid rests only when infinitely far removed from the falling cylinder. As an approximation it will be assumed that the fluid rests at a distance δR from the cylinder. Using this assumption, the flow domain is divided as shown in Figure 1 where the fluid rests in domains 6 and 7, and the velocity distributions in domains (1,2,3,4,5) and (1′,2′,3′,4′,5′) are identical due to the axisymmetric property. For a coordinate system moving with the center of the cylinder, the boundary conditions for the

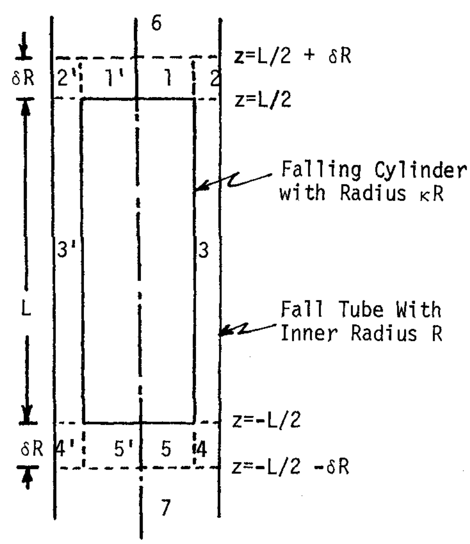

Fig. 1. Falling cylinder viscometer with divided flow domains.

Correspondence concerning this paper should be addressed to G. W. Swift. M. C. S. Chen is with Internation Petrodata, Inc., Calgary, Alberta, Canada.

solution of Equations (1), (2), and (3) are:

$$\left.\begin{array}{ll} v_r = 0,\ v_z = v_1 & @\ z = \pm(\delta R + L/2) \\ v_z = 0 & @\ z = \pm L/2 \text{ and } r \leq \kappa R \\ v_r = v_z = 0 & @\ -L/2 \leq z \leq L/2 \text{ and } r = \kappa R \\ v_r = 0,\ v_z = v_1 & @\ r = R \text{ for all } z \end{array}\right\} \tag{8}$$

For $N_{Re} << 1$, the convective terms are negligible and Equations (1), (2), and (3) become a linear set. Ritz' method (7) then applies, and, if the trial velocity distribution function satisfies Equation (1), the solution is achieved when $\overline{F}_k$ is a minimum.

If the convective terms cannot be neglected, the classical variational calculus fails. However, according to Schechter (9), a local potential method can be applied to Equations (1), (2), and (3) and the solution achieved when I_k is a minimum:

$$I_k = \iint [-2\rho\{(v_r^0)^2(\partial v_r/\partial r) + (v_z^0)^2(\partial v_z/\partial z) + v_r^0 v_z^0(\partial v_z/\partial r + \partial v_r/\partial z)\} + \mu\{2[(\partial v_r/\partial r)^2 + (v_r/r)^2 + (\partial v_z/\partial z)^2] + (\partial v_r/\partial z + \partial v_z/\partial r)^2\}]2\pi r dr dz \tag{9}$$

It is assumed that the functions with superscript 0 are evaluated at a stationary state not subject to variation; those without superscript 0 are varied. The approximate solution will be obtained when the two functions are equal.

The details of the solution methods for creeping and noncreeping flow and the computer programs used to implement the methods are presented in Chen's dissertation (4).

The results of the calculations for creeping and noncreeping flow are given in Table 1 where Ψ_{ee} is presented as a function of N_{Re}, κ, and $L/2R$. The creeping flow results in this table correspond to the values presented for $N_{Re} = 0$.

The key to the successful use of the variational method is the selection of proper trial function. In the cases studied above, the trial velocity distributions, using up to eight parameters, were computed to test for convergence. For creeping flow, convergence was excellent. The extension to noncreeping flow agrees with the creeping flow results at low N_{Re} but, for $N_{Re} > 100$, is not convergent even for an eight parameter trial function (see Figure 2). Computations for trial functions with more than eight parameters were not attempted because of the excessive computer time required.

TABLE 1. Ψ_{ee} AS A FUNCTION OF N_{Re}, κ, AND $L/2R$

		Ψ_{ee}				
N_{Re}	κ	L/2R = 2	L/2R = 4	L/2R = 6	L/2R = 8	L/2R = 12
0	0.8489	0.9451	0.9718	0.9810	0.9857	0.9904
1		0.9451	0.9718	0.9810	0.9857	
5		0.9451	0.9718	0.9810	0.9857	
10		0.9450	0.9717	0.9810	0.9857	
25		0.9444	0.9714	0.9808	0.9855	
50		0.9423	0.9703	0.9800	0.9849	
75		0.9387	0.9684	0.9787	0.9839	
100		0.9332	0.9655	0.9767	0.9824	
0	0.8999	0.9619	0.9806	0.9870	0.9902	0.9934
1		0.9619	0.9806	0.9870	0.9902	
5		0.9619	0.9806	0.9870	0.9902	
10		0.9619	0.9806	0.9870	0.9902	
25		0.9616	0.9804	0.9869	0.9901	
40		0.9612	0.9802	0.9867	0.9900	
60		0.9604	0.9798	0.9865	0.9898	
80		0.9596	0.9794	0.9862	0.9896	
100		0.9588	0.9790	0.9859	0.9894	
0	0.9210	0.9691	0.9843	0.9895	0.9921	0.9947
1		0.9692	0.9844	0.9895	0.9921	
5		0.9692	0.9844	0.9895	0.9921	
10		0.9692	0.9844	0.9895	0.9921	
25		0.9685	0.9840	0.9893	0.9919	
50		0.9685	0.9840	0.9893	0.9919	
75		0.9684	0.9840	0.9892	0.9919	
100		0.9684	0.9839	0.9892	0.9919	

TABLE 2. VISCOSITY AND DENSITY OF OILS USED IN EXPERIMENTS AS CERTIFIED BY CANNON INSTRUMENT COMPANY AT 25°C.

Oil Number	Viscosity, cp.	Density, g./cu. cm.
S-2000	5137	0.8749
S-200	388.1	0.8736
S-20	31.41	0.8664
S-6	7.910	0.8592

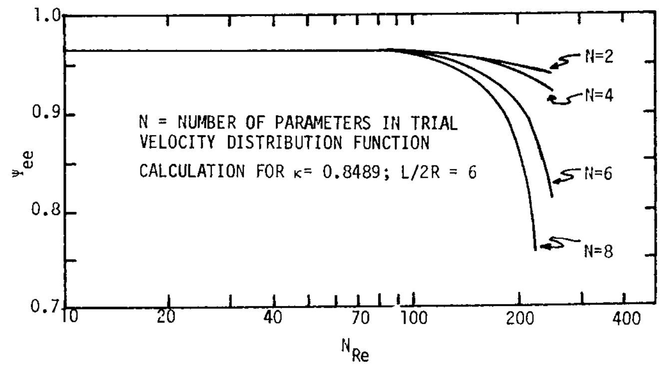

Fig. 2. Ψ_{ee} versus N_{Re} with variation in number of parameters N used.

EXPERIMENT

Laboratory tests were conducted to compare experiment with theory. Theory predicts that

$$v_1 = v_0\Psi_{ee} = \beta_0\Psi_{ee}g(\sigma - \rho)/\mu \tag{10}$$

while experimentally

$$v_2\mu/[g(\sigma - \rho)] = \beta_2 \tag{11}$$

Thus, by comparing

$$v_2/v_1 = \beta_2/(\beta_0\Psi_{ee}) = \beta_r/\Psi_{ee} \tag{12}$$

the success of the theoretical calculation is established if $v_2/v_1 = 0$. This presumes, of course, that the viscometer is designed so that eccentricity is minimized [see Chen et al. (3)] and construction details such as alignment pins, etc. do not significantly change the terminal velocity.

Apparatus and Procedure

The appartus, described in detail by Chen (4), consisted of a pyrex tube (1.0000 ± 0.0002-in. diam. by 24 in. long) immersed in a thermostat controlled at 25 ± 0.025°C. The tube was filled with one of the standard viscosity oils listed in Table 2 and stainless steel cylinders, the density of which could be varied by adding mercury, were timed while falling at terminal velocity through the oil. Three test cylinders of diameters 0.8489, 0.8999, and 0.9210 ± 0.0001 in. and initially 12 in. in length were employed in the experiments (see Figure 3 for construction details). Each cylinder was carefully fitted with brass alignment pins to insure that error from eccentricity was less than 0.1%. After each series of experiments, the cylinders were disassembled to shorten the length, and then, because of the method of construction, reassembled without disturbing the alignment pin positions. During the various series of experiments, the viscosities of the oils were periodically checked to determine that the oil viscosity was not changing.

RESULTS AND DISCUSSION

Figures 4 and 5 present $v_2/v_1 = \beta_r\Psi_{ee}$ for creeping flow. These figures show that the experimental error as judged by repeatability is approximately 0.5%. Further, by comparing the data for the three different cylinders at the same length, it can be seen that there is no change in the pin alignments during the course of the experimental work. Comparison of the data for the two oils used in the creeping flow experiments (data of Figure 4 versus those of Figure 5) shows a rather constant disagreement of about 0.5%. The most likely reason for this is an error in the absolute viscosity of one (or both) of the oils used. By averaging the two sets of data over the range of $L/2R$ studied, the ratio of β_r/Ψ_{ee} is almost constant for $L/2R$ = 6, 8, 12 at a value of 0.997. That this ratio is less than unity, which would be a perfect test of the theory, is most likely due to friction of the alignment pins which will cause the experimental terminal velocity to be less than the theoretical value. β_r/Ψ_{ee} increases rather rapidly with decreasing $L/2R$ *for* $L/2R$ less than 6 indicating that the theory developed cannot be applied to falling cylinder viscometers for $L/2R < 6$.

The experimental data obtained for noncreeping flow are compared with theory in Figure 6. Data for $L/2R < 6$ are excluded based on the remarks of the preceding paragraph. β_r/Ψ_{ee} decreases with increasing N_{Re} and exceeds the repeatability of the experiments (0.5%) at $N_{Re} \simeq 25$. This indicates that the effect of turbulence in the viscometer sets in earlier than predicted by theory and can best be explained by the fact that theory does not account for the alignment pin contribution to turbulence. Thus the utility of the theory developed in noncreeping flow is limited, preferably to N_{Re} less than 10.

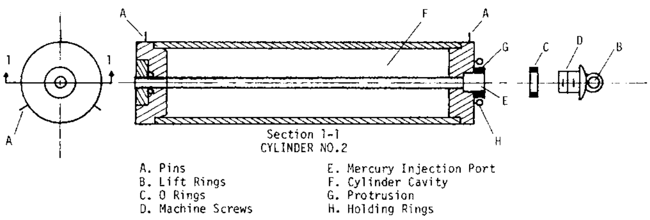

Fig. 3. Variable density falling cylinder viscometer.

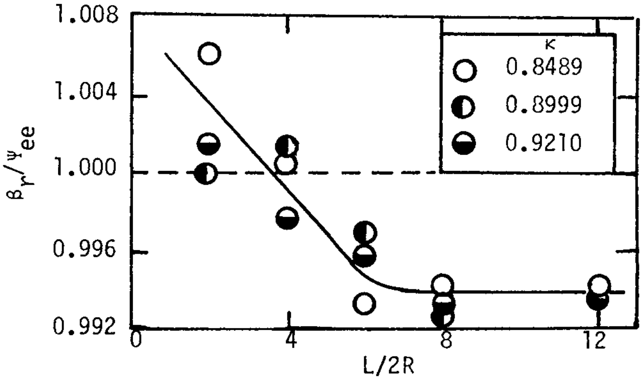

Fig. 4. β_r/Ψ_{ee} **versus** $L/2R$ **for Oil S-2000 @** $N_{Re} < 1$.

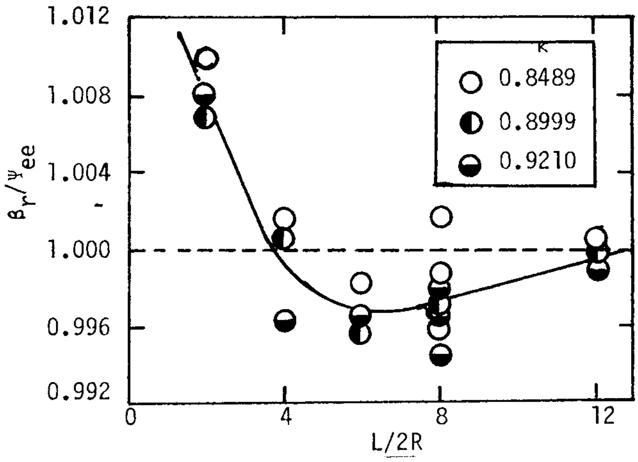

Fig. 5. β_r/Ψ_{ee} **versus** $L/2R$ **for Oil S-200 @** $N_{Re} < 1$.

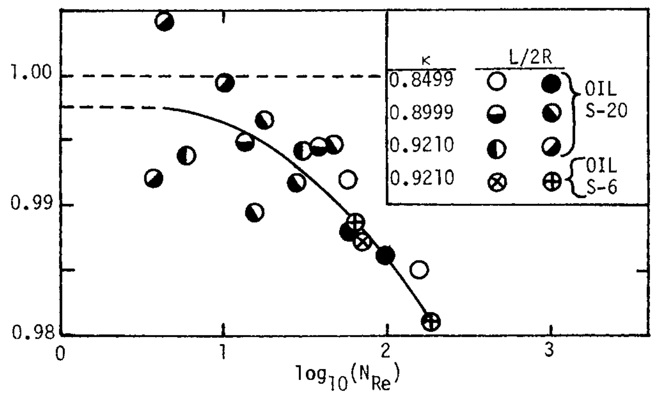

Fig. 6. β_r/Ψ_{ee} **versus** N_{Re} **for noncreeping flow.**

CONCLUSIONS

The theoretical end effect correction has been calculated for the falling cylinder viscometer in both creeping and non-creeping flow. The calculated correction is converged to within 0.1% for creeping flow and appears to be converged for noncreeping flow for $N_{Re} < 100$. Experimental results for three viscometers agree with theory for $N_{Re} <$ 25 within 0.5%. In creeping flow, pin friction probably accounts for the disagreement (approximately 0.3%). In noncreeping flow, theory does not predict the proper point of onset of turbulence, probably because flow past the pins controls.

ACKNOWLEDGMENTS

Financial support for M. C. S. Chen was provided under NSF Grant GK-4193. Computer time was furnished through the Computation Center of the University of Kansas.

NOTATION

d = total differential, dimensionless
∂ = partial differential, dimensionless
$\overline{F}_k$ = kinetic force, dimensionless
g = acceleration of gravity, 979.99 cm./sec.^{2} at experimental location
I_k = integral defined by Equation (9), g./(cm.) (sec.)^3
L = length of falling cylinder, cm.

N_{Re} = Reynolds number = $2Rv\rho/\mu$, dimensionless
p = pressure, dyne/sq.cm.
r = radius, cm.
R = radius of fall tube, cm.
v_r, v_r^0, v_z, v_z^0 = axisymmetric cylindrical velocity component, cm./sec.
v_0 = theoretical terminal velocity without end effects, cm./sec.
v_1 = theoretical terminal velocity with end effects, cm./sec.
v_2 = experimental terminal velocity, cm./sec.
z = distance, cm.

Greek Letters

β_0 = viscometer constant, theoretical, sq.cm.
β_2 = viscometer constant, experimental, sq.cm.
β_r = viscometer constant, reduced, dimensionless
κ = radius of falling cylinder/radius of fall tube, dimensionless
μ = viscosity, g./(cm.)(sec.)
ρ = density of oil, g./cu.cm.
σ = density of cylinder, g./cu.cm.
Φ_v' = axisymmetric velocity dissipation function, 1/sec.^{2}
Ψ_{ee} = theoretical end effects coefficient, dimensionless

LITERATURE CITED

1. Ashare, Edward, R. B. Bird, and J. A. Lescarboura, *AIChE J.*, **11**, 910 (1965).
2. Bird, R. B., W. E. Stewart, and E. N. Lightfoot, "Transport Phenomena," Wiley, N.Y. (1964).
3. Chen, M. C. S., J. A. Lescarboura, and G. W. Swift, *AIChE J.*, **14**, 123 (1968).
4. Chen, M. C. S., Ph.D. dissertation, Univ. Kansas, Lawrence (1970).
5. Eichstadt, F. J., and G. W. Swift, *AIChE J.*, **12**, 1179 (1966).
6. Huang, E. T. S., G. W. Swift, and F. Kurata, *AIChE J.*, **12**, 932 (1966).
7. Kantorovich, L. V., and V. I. Krylov, "Approximate Methods of Higher Analysis," Interscience, N.Y. (1958).
8. Lohrenz, J., G. W. Swift, and F. Kurata, *AIChE J.*, **6**, 547 (1960).
9. Schechter, R. S., "The Variational Method in Engineering," McGraw-Hill, N.Y. (1967).
10. Swift, G. W., J. Lohrenz, and F. Kurata, *AIChE J.*, **6**, 415 (1960).
11. Walker, J. D., Ph.D. dissertation, Univ. Kansas, Lawrence (1970).

Manuscript received May 28, 1970; revision received July 16, 1971; paper accepted August 2, 1971.

Non-Newtonian Behavior of a Suspension of Liquid Drops in Tube Flow

W. A. HYMAN and RICHARD SKALAK

Department of Civil Engineering and Engineering Mechanics
Columbia University, New York, New York 10027

This paper presents an analysis and computed results of the flow of deformable droplets of one Newtonian fluid suspended in another Newtonian fluid. Surface tension is assumed to act at the interface of the two fluids. Non-Newtonian characteristics of the suspension are demonstrated and are qualitatively similar to flow characteristics of blood in capillaries.

The results show that the deformation of the drops may result in a significant reduction in the pressure gradient compared with that necessary for a suspension of rigid spheres or spherical (nondeformable) liquid drops. The decrease in the pressure gradient is velocity dependent. This constitutes a mechanism of non-Newtonian behavior of the suspension as a whole, and is attributable to the flexibility of the suspended elements. The resultant shapes of the liquid drops are similar to the shapes of red blood cells that have been observed in narrow glass capillaries as well as in blood vessels.

This study considers the axisymmetric flow of a suspension of deformable liquid drops through a rigid cylindrical tube (Figure 1). The liquid in each drop and the suspending fluid are both assumed to be Newtonian and incompressible. A surface tension is assumed to act at the interface. The analysis allows for an arbitrary ratio of viscosity of the liquid drops to that of the suspending fluid. The motion is assumed to be sufficiently slow so that inertial terms in the equation of motion may be neglected.

This system is considered to be a possible model of blood flow in the capillaries. The liquid drops of the present

W. A. Hyman is at the Department of Mechanical Engineering, Massachusetts Institute of Technology, Cambridge, Massachusetts 02139.